PRELIMINARY RESULTS FOR EXCLUSIVE $b \to u\ell\nu$ DECAYS FROM CLEO

Lawrence Gibbons
University of Rochester, Rochester, NY 14627

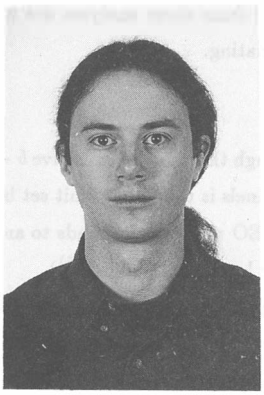

Abstract

A preliminary analysis of exclusive $b \to u\ell\nu$ decays to the final states $\pi^{\mp}\ell^{\pm}\nu$, $\pi^0\ell^{\pm}\nu$, $\rho^{\mp}\ell^{\pm}\nu$, $\rho^0\ell^{\pm}\nu$ and $\omega\ell^{\pm}\nu$ based on 2.2×10^6 $B\bar{B}$ decays collected at CLEO is presented. We have measured the first exclusive $b \to u\ell\nu$ branching fraction $\mathcal{B}(B^0 \to \pi^-\ell^+\nu) = [1.19 \pm 0.41 \pm 0.21 \pm 0.19] \times 10^{-4}$ ($[1.70 \pm 0.51 \pm 0.31 \pm 0.27] \times 10^{-4}$), with the ISGW (WSB) model used for efficiency determination. A 90% C.L. upper limit on $\mathcal{B}(B^0 \to \rho^-\ell^+\nu)$ similar to the previous CLEO limit is obtained. The ratio $\Gamma(B^0 \to \rho^-\ell^+\nu)/\Gamma(B^0 \to \pi^-\ell^+\nu) < 3.4$ at the 90% confidence level for both the ISGW and WSB models. This ratio provides some discrimination between form factor models.

1 Introduction

This talk will focus on a preliminary CLEO analysis of $b \to u\ell\nu$ decays to the exclusive final states $\pi\ell\nu$, $\rho\ell\nu$ and $\omega\ell\nu$. The ultimate goal of this analysis is to improve our knowledge of $|V_{ub}|$. ARGUS[1] and CLEO[2] have already demonstrated that $|V_{ub}| > 0$ by examining the inclusive lepton momentum spectrum from B decays at the $\Upsilon(4S)$. They observe events beyond 2.4 GeV/c, which is kinematically forbidden for the copious $b \to c\ell\nu$ processes, but is still accessible to $b \to u\ell\nu$ decays. While these analyses clearly establish an excess in this endpoint region, and hence that $|V_{ub}| > 0$, extracting a reliable value of $|V_{ub}|$ is difficult because of the theoretical uncertainty in extrapolating from the observed rate in the endpoint region to the total $b \to u\ell\nu$ rate. Values of $|V_{ub}/V_{cb}|$ obtained from these analyses are now in the 7% to 11% range, with the theoretical uncertainty dominating.

2 Exclusive $b \to u\ell\nu$

An alternate route to $|V_{ub}|$ is through the study of exclusive $b \to u\ell\nu$ channels. The best previous information concerning such channels is the upper limit set by CLEO[4] in the combined modes $\rho^-\ell^+\nu$, $\rho^0\ell^+\nu$ and $\omega\ell^+\nu$. The CLEO result corresponds to an upper limit of $\mathcal{B}(B^0 \to \rho^-\ell^+\nu) < 3.2 \times 10^{-4}$ at the 90% confidence level (ISGW model[5]).

The preliminary analysis presented here studies the two pseudoscalar modes $\pi^-\ell^+\nu$ and $\pi^0\ell^+\nu$, the three vector modes $\rho^-\ell^+\nu$, $\rho^0\ell^+\nu$ and $\omega\ell^+\nu$, and the charge conjugate modes. At a fixed $|V_{ub}|$, the existing form factor models predict a wide range of partial widths for these modes, as Table 1 shows. Unfortunately, measured branching fractions depend on the form factor model used to evaluate the experimental efficiencies, as does the extraction of $|V_{ub}|$. We therefore need to discriminate between the different models.

The ratio $\Gamma(B^0 \to \rho^-\ell^+\nu)/\Gamma(B^0 \to \pi^-\ell^+\nu)$ provides one means of discrimination. Because the $\pi\ell\nu$ rate is helicity-suppressed when the daughter meson is at rest in the B meson rest frame (at q^2_{max}), where the form factors for the decay are largest, while the $\rho\ell\nu$ rate is not, we expect the ratio to be larger than one. The exact value for the ratio will depend on the q^2-behavior of the form factors. In Table 1, we see that the predictions of the ratio span a fairly

Table 1: Predictions for the exclusive partial widths $\Gamma(B^0 \to \pi^-\ell^+\nu)$ and $\Gamma(B^0 \to \rho^-\ell^+\nu)$ and the ratio $\Gamma(B^0 \to \rho^-\ell^+\nu)/\Gamma(B^0 \to \pi^-\ell^+\nu)$. The partial width units are $10^{12}|V_{ub}|^2$ sec^{-1}.

Model	$\Gamma(B^0 \to \pi^-\ell^+\nu)$	$\Gamma(B^0 \to \rho^-\ell^+\nu)$	$\Gamma(B^0 \to \rho^-\ell^+\nu)/\Gamma(B^0 \to \pi^-\ell^+\nu)$
WSB[6]	6.3 – 10.0	18.7 – 42.5	3.0 – 4.3
KS[7]	7.25	33.0	4.6
ISGW[5]	2.1	8.3	4.0
ISGW II[8]	9.6	14.2	1.5

broad range, so the ratio should prove useful.

3 Neutrino "Measurement" and Exclusive $b \to u\ell\nu$

Experimentally, semileptonic decays are troublesome because of the undetected neutrino. This analysis takes advantage of the excellent hermeticity and resolution of the CLEO II detector located at the Cornell Electron Storage Ring (CESR) to obtain information about the neutrino in semileptonic $b \to u\ell\nu$ decays. Three concentric tracking devices provide a momentum resolution of $\sigma_p/p = 0.005 \oplus 0.0015p$ (p in GeV/c), while covering 95% of the 4π solid angle. The CsI calorimeter located inside of the CLEO solenoid provides an energy resolution well approximated by $\sigma_E/E = 0.019 + 0.0035/E^{0.75} - 0.001E$ (E in GeV), while covering 98% of 4π. The detector is described in detail elsewhere.[9] This analysis is based on a data sample with a luminosity of 2.09 fb^{-1} (about 2.2×10^6 $B\bar{B}$ decays).

The underlying idea is very simple: the $B\bar{B}$ system is at rest at CLEO and the beam energy is known very precisely, so we can "measure" the neutrino four momentum by measuring the missing energy and momentum of an event. We define

$$E_{miss} \equiv 2E_{beam} - \sum_i E_i \quad (1)$$

$$\vec{p}_{miss} \equiv -\sum_i \vec{p}_i, \quad (2)$$

where the index i runs over all charged tracks and all showers in the calorimeter that pass cuts designed to reject false tracks and spurious showers from hadronic interactions.

In events with no extra missing particles, $\vec{p}_{miss}$ can be reliably associated with the momentum $\vec{p}_\nu$ of the signal mode neutrino. The $b \to u\ell\nu$ decay can then be fully reconstructed: the energy difference $\Delta E \equiv E_{beam} - (E_h + E_\ell + |\vec{p}_\nu|)$, where h is the candidate hadron, should be zero, and the beam-energy constrained mass $m_B \equiv \sqrt{E^2_{beam} - |\vec{p}_h + \vec{p}_\ell + \vec{p}_\nu|^2}$ should reconstruct at the B mass. Signal events that are reconstructible show resolutions of approximately 260 MeV on E_{miss} and 110 MeV on $|\vec{p}_{miss}|$.

Signal events with particles missing in addition to the neutrino usually fail the reconstruction criteria. On the other hand, those background events that pass the criteria do so because they have extra particles missing. Consequently, we reject events with multiple leptons or a non-zero total charge because they indicate a second neutrino or a missed charged particle, respectively. Most remaining events with extra missing particles are eliminated by requiring that $M^2_{miss} \equiv E^2_{miss} - |\vec{p}_{miss}|^2$ be consistent with zero. The criterion $M^2_{miss}/2E_{miss} < 350$ MeV is used since the M^2_{miss} resolution varies approximately as $2E_{miss}\sigma_{E_{miss}}$.

Continuum background is suppressed using standard event shape variables. The $b \to u\ell\nu$ processes are enhanced over $b \to c$ by requiring the leptons to have momenta larger than 1.5

GeV/c (2.0 GeV/c) in the $\pi\ell\nu$ (vector) modes. The lower cut is used in the π modes because these modes are expected to have a softer lepton momentum spectrum.

Both electrons and muons are used in this analysis. We combine information from specific ionization, energy/momentum measurements from the calorimeter and tracking systems, and position matching from these two systems to identify electrons down to 600 MeV/c. Muon candidates must register hits in muon counters at least 5 interaction lengths deep, limiting the muon momentum range to approximately 1.4 GeV/c. The probability that a hadron is misidentified as a lepton (a "fake lepton") is of the order 0.1% (1%) for electron (muon) identification.

Candidate 2π (3π) combinations must have an invariant mass within 90 (30) MeV of the nominal ρ (ω) mass. A π^0 candidate must have a 2-photon invariant mass within 2 standard deviations (about 12 MeV) of the π^0 mass. Within any one of the five modes, we pick the meson candidate in each event that yields the smallest value of $|\Delta E|$.

We require the lepton, neutrino and meson candidates to satisfy -250 MeV $< \Delta E <$ 150 MeV. The cut is asymmetric because the $b \to c$ backgrounds increase rapidly as ΔE increases. The range 5.265 GeV $< m_B <$ 5.2875 GeV defines the signal region. The m_B distribution for data after all cuts, including the ΔE cut, is shown in Figure 1 for the combination of the $\pi^{\mp}\ell^{\pm}\nu$ and $\pi^0\ell^{\pm}\nu$ modes, and for the combination of the three vector modes. There is a clear excess above the background in the signal region for the $\pi\ell\nu$ modes. The fit yielding the background levels shown is described in the next section.

The dominant background in both the π and the vector modes comes from $b \to c\ell\nu$ decays in events containing either an undetected K_L or a second neutrino. The small backgrounds in each mode from fake leptons and from continuum processes are measured with the data. In the π modes, Monte Carlo studies indicate that feed-across from the $\rho\ell\nu$ modes should contribute the next largest background. In the vector modes, $b \to u\ell\nu$ decays to higher mass and non-resonant final states form the other major background component. Our fits do not make any requirement on the distribution of events inside our mass windows, so resonant and non-resonant final states are not distinguished. Consequently only an upper limit on $\mathcal{B}(B^0 \to \rho^-\ell^+\nu)$ will be obtained. We derive the limit conservatively by assuming zero background from the non-resonant and higher mass decays.

4 Extracting the Yields

After subtracting the continuum and fake lepton backgrounds, we fit the beam-constrained mass distributions in our five reconstructed $b \to u\ell\nu$ modes simultaneously, which allows the data in the vector modes to constrain the $\rho\ell\nu$ background in the $\pi\ell\nu$ modes. In addition to the signal shapes and the feed-across shapes between the five modes, the fit includes $b \to c$ and other

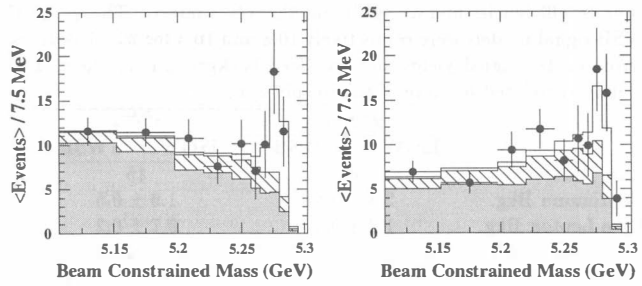

Figure 1: Beam constrained mass distributions for the combined $\pi^-\ell^+\nu$ and $\pi^0\ell^+\nu$ modes (left) and the combined vector modes (right). The points are continuum- and fake-subtracted data. The histograms show the contribution from $b \to c$ (shaded), $u\ell\nu$ crossfeed (hatched) and signal (hollow).

$b \to u\ell\nu$ background components. The isospin relations $\frac{1}{2}\Gamma(B^0 \to \pi^-\ell^+\nu) = \Gamma(B^+ \to \pi^0\ell^+\nu)$ and $\frac{1}{2}\Gamma(B^0 \to \rho^-\ell^+\nu) = \Gamma(B^+ \to \rho^0\ell^+\nu) \approx \Gamma(B^+ \to \omega\ell^+\nu)$ constrain the neutral meson rates relative to the charged meson rates. We therefore obtain two yields, $N_{\pi^\pm\ell^\mp\nu}$ and $N_{\rho^\pm\ell^\mp\nu}$, from the fit.

The $b \to c\ell\nu$ and feed-across background shapes in m_B are obtained from Monte Carlo simulation. The $b \to c\ell\nu$ background level floats independently in each of the five modes, while the feed-across rates between the five modes are tied to the signal yields $N_{\pi^\pm\ell^\mp\nu}$ and $N_{\rho^\pm\ell^\mp\nu}$.

Monte Carlo simulation also provides the m_B distributions for the non-resonant and higher mass $b \to u\ell\nu$ backgrounds. The inclusive lepton yield at high momentum fixes this background level. We vary the physical model and the rate by hand to estimate the systematic uncertainty in this procedure.

The results of the fit from which the $\pi\ell\nu$ yield (and the background levels in Figure 1) is obtained are summarized in Table 2. The efficiencies and crossfeed probabilities have been determined using the ISGW and WSB models. We obtain similar $\pi\ell\nu$ yields for the two models, but obtain efficiencies that differ by approximately 30%. The $b \to c\ell\nu$ background levels in the five modes are all consistent with absolute Monte Carlo predictions based on the luminosity. Correcting for acceptance and averaging the electron and muon samples, we obtain the preliminary branching fraction $\mathcal{B}(B^0 \to \pi^-\ell^+\nu) = [1.19 \pm 0.41] \times 10^{-4}$ ($[1.70 \pm 0.55] \times 10^{-4}$) for the ISGW (WSB) model, where the errors are statistical only. We obtain consistent results if we fit using the ΔE distributions, having resolved multiple candidates using m_B.

To obtain upper limits for the vector modes, we perform a similar fit assuming no non-resonant or higher mass $b \to u\ell\nu$ backgrounds. This fit gives the same $\pi\ell\nu$ yield. We obtain the efficiency-corrected numbers of 834 ± 337 (1248 ± 484) $\rho^\mp\ell^\pm\nu$ decays for the ISGW (WSB)

Table 2: Backgrounds, efficiencies and fit results for the $\pi\ell\nu$ analysis. The χ^2 for the fits using the ISGW and WSB signal models were respectively 10.8 and 10.3 for $20-7$ degrees of freedom. Note that the errors on the signal yields and crossfeed backgrounds in the $\pi^-\ell^+\nu$ and $\pi^0\ell^+\nu$ modes are completely correlated because of the isospin constraints.

	$\pi^-\ell^+\nu$		$\pi^0\ell^+\nu$	
	ISGW	WSB	ISGW	WSB
Raw Data	30		15	
Continuum Bkg.	2.3 ± 0.8		1.0 ± 0.5	
Fake Lepton Bkg.	1.2 ± 0.3		0.7 ± 0.2	
other $u\ell\nu$ Bkg.	0.6		0.2	
Efficiency	2.9%	2.1%	1.9%	1.4%
Signal Yield	15.6 ± 5.3	16.3 ± 5.3	5.0 ± 1.7	5.3 ± 1.7
$b \to c$ Bkg.	9.8 ± 1.1	9.8 ± 1.1	1.8 ± 0.5	1.7 ± 0.5
ρ/ω Bkg.	3.8 ± 1.7	3.4 ± 1.4	1.8 ± 0.8	1.6 ± 0.7

model, and a $\Gamma(B^0 \to \rho^-\ell^+\nu)/\Gamma(B^0 \to \pi^-\ell^+\nu)$ ratio of $1.56^{+1.29}_{-0.76}$ ($1.63^{+1.21}_{-0.75}$).

Many distributions have been examined for consistency with the $\pi\ell\nu$ hypothesis. The charged lepton momentum spectrum for $\pi^\mp\ell^\pm\nu$ and $\pi^0\ell^\pm\nu$ candidates in the m_B signal region is shown in Figure 2. The spectrum obtained from the data is quite stiff, with a sizeable fraction of events beyond the $b \to c\ell\nu$ endpoint. The sum of the signal and background distributions, scaled according to the fit results, shows good agreement with the data. The π and ν momentum spectra are also consistent with the results of the fit.

For $B \to \pi\ell\nu$, the $V-A$ interaction predicts that the angle between the π and the lepton in the W rest frame, $\theta^*_{\pi\ell}$, should have a $\sin^2\theta^*_{\pi\ell}$ distribution. The observed $\cos\theta^*_{\pi\ell}$ distribution, also shown in Figure 2, is in good agreement with this expectation. We estimate the probability, including systematic uncertainties, that the background processes could fluctuate to give the

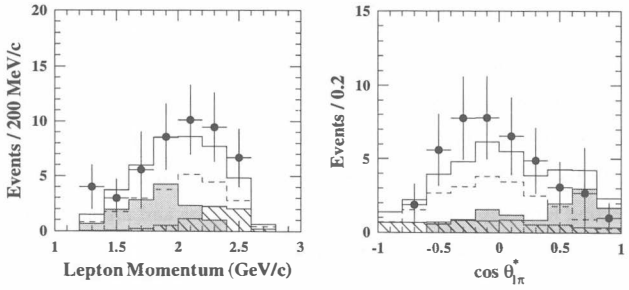

Figure 2: Charged lepton spectrum (left) and $\cos\theta^*_{\pi\ell}$ distribution (right) for the combined $\pi^-\ell^+\nu$ and $\pi^0\ell^+\nu$ modes. The points are continuum- and fake-subtracted data. The top histogram is the total prediction using rates from the yield fit, with components $b \to c$ (shaded), $u\ell\nu$ crossfeed (hatched) and signal (dashed).

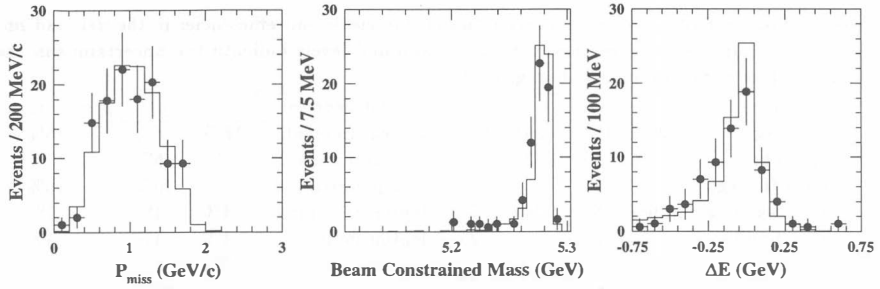

Figure 3: $|\vec{p}_{miss}|$ spectrum (left) m_B distribution (center) and ΔE distribution (right) for $D^{*\pm}\ell^{\mp}\nu$ reconstruction. The points are continuum and combinatoric background-subtracted data. The histograms are signal Monte Carlo distributions normalized to equal area.

observed m_B and $\cos\theta^*_{\pi\ell}$ distributions in the combined $\pi\ell\nu$ modes, and obtain 6.4×10^{-5}. This corresponds to a 3.8 standard deviation significance for a Gaussian distribution.

5 Systematics

The systematic uncertainties on the yields and efficiencies are summarized in Table 3. The dominant uncertainty in the yields comes from the uncertainty in the shapes of the background m_B distributions. The shapes have been checked in a variety of ways: examining the shapes in ΔE sidebands and in signal-free modes (eg., $K_S\ell\nu$), and varying the misreconstruction behavior of the Monte Carlo simulation.

The uncertainty in the efficiencies is dominated by the neutrino-measurement simulation. One method of estimating this uncertainty is to use this technique to measure the branching fraction for $B \to D^{*\pm}\ell^{\mp}\nu$ via the modes $D^{*\pm} \to \pi^{\pm}D^0$, $D^0 \to K^{\mp}\pi^{\pm}$. We find that the simulation of E_{miss}, $\vec{p}_{miss}$, ΔE and m_B agrees well with the data (Figure 3), and that $\mathcal{B}(B^0 \to D^{*-}\ell^+\nu) = 4.66 \pm 0.65\%$. This agrees with the published CLEO result[10] of $4.49 \pm 0.32 \pm 0.32\%$, which used a higher statistics technique. The 15% statistical uncertainty is taken as the systematic uncertainty; other studies indicate that this is a conservative estimate. We expect this systematic to cancel in the ρ/π ratio, but retain a preliminary 15% uncertainty.

6 Conclusion

Combining the $\pi\ell\nu$ yields and the systematic uncertainties, we obtain the preliminary branching fraction $\mathcal{B}(B^0 \to \pi^-\ell^+\nu) = [1.19 \pm 0.41 \pm 0.21 \pm 0.19] \times 10^{-4}$ ($[1.70 \pm 0.51 \pm 0.31 \pm 0.27] \times 10^{-4}$) using the ISGW (WSB) model to evaluate efficiencies. The errors are statistical, systematic on the yield, and systematic on the efficiency, respectively. This is the first measurement of any exclusive $b \to u\ell\nu$ branching fraction. The probability of a background fluctuation resulting in

Table 3: Summary of systematic uncertainties on the yields and efficiencies in the $\pi\ell\nu$ and $\rho\ell\nu$ modes. The numbers in parentheses in the background levels indicate the uncertainty in the background as a fraction of that background.

On yields:	$\pi\ell\nu$		$\rho\ell\nu$		On Efficiencies:	$\pi\ell\nu$	$\rho\ell\nu$	ρ/π ratio
$b \to c$ bkg.	(20%)	13%	(20%)	23%	ν-measurement	15%	15%	15%
$\rho/\omega\ell\nu$ bkg.	(36%)	8%	(63%)	7%	$\pi/\rho/\omega$ finding	3%	6%	7%
other $u\ell\nu$ bkg.		8%		—	ρ/ω polarization	—	10%	10%
cont.+fake bkg.	(20%)	6%	(24%)	7%	lepton fake rates	4%	4%	4%
lepton finding		2%		2%	lepton finding	4%	4%	4%
					Luminosity	2%	2%	—
Total		**18%**		**25%**	**Total**	**16%**	**20%**	**20%**

the observed signal is 6.4×10^{-5}.

Assuming no non-resonant or high mass $u\ell\nu$ background, we obtain a conservative 90% C.L. upper limit of $\mathcal{B}(B^0 \to \rho^-\ell^+\nu) < 3.1 \times 10^{-4}$ for the ISGW model and $\mathcal{B}(B^0 \to \rho^-\ell^+\nu) < 4.6 \times 10^{-4}$ for the WSB model. The statistical and systematic uncertainties have been combined in quadrature in evaluating these limits. The results are comparable to the previous CLEO upper limits for the vector modes.

Finally, we find $\Gamma(B^0 \to \rho^-\ell^+\nu)/\Gamma(B^0 \to \pi^-\ell^+\nu) < 3.4$ at the 90% confidence level for both the ISGW and WSB models. Again, statistical and systematic uncertainties have been combined in quadrature. Comparing to the predictions in Table 1, the WSB model is compatible with this limit, but it is difficult to reconcile the ISGW model with this limit.

These preliminary measurements herald a new era for the study of V_{ub}. CLEO is still refining these measurements, with 50% more data soon to be available and work in progress on the separation of the vector modes from non-resonant modes.

7 References

1. H. Albrecht *et al.* (ARGUS collaboration), Phys. Lett. **B234**, 409 (1990); *Ibid*, Phys. Lett. **B255**, 297 (1991).
2. R. Fulton *et al.* (CLEO collaboration), Phys. Rev. Lett. **64**, 16 (1990); J. Bartelt *et al.* (CLEO collaboration), Phys. Rev. Lett. **71**, 4111 (1993).
3. G. Altarelli *et al.*, Nucl. Phys. **B208**, 365 (1982).
4. A.Bean *et al.* (CLEO collaboration), Phys. Rev. Lett. **70**, 2681 (1993).
5. N.Isgur, D.Scora, B.Grinstein and M.Wise, Phys. Rev. **D39**, 799 (1989).
6. M.Wirbel, B.Stech and M.Bauer, Z. Phys. **C29**, 637 (1985).
7. J.G.Körner and G.A.Schuler, Z. Phys. **C38**, 511, (1988).
8. N.Isgur and D.Scora, CEBAF preprint CEBAF-TH-94-14.
9. Y. Kubota *et al.* (CLEO collaboration), Nucl. Instrum. Methods Phys. Res. Sect. A **320**, 66 (1992).
10. B. Barish *et al.* (CLEO collaboration), Phys. Rev. **D51**, 1014 (1995).